ACS APPLIED MATERIALS & INTERFACES

Research Article

Cite This: ACS Appl. Mater. Interfaces 2018, 10, 13100−13106

www.acsami.org

Effects of Melanin on Optical Behavior of Polymer: From Natural Pigment to Materials Applications

Yang Wang, Xuefei Wang, Ting Li, Piming Ma, Shengwen Zhang, Mingliang Du, Weifu Dong,* Yi Xie, and Mingqing Chen

Key Laboratory of Synthetic and Biological Colloids, Ministry of Education, School of Chemical and Material Engineering, Jiangnan University, 1800 Lihu Road, Wuxi 214122, China

ABSTRACT: Melanin is a kind of ubiquitous natural pigment, which serves a variety of protective functions in many organisms. In the present study, natural melanin and synthetic melanin nanoparticles (NPs) were systematically investigated for its potential application in polymeric optical materials. A significant short-wavelength shielding and high visible light transparency polymer nanocomposite was easily obtained via tuning the melanin particle size. In particular, the nanocomposite film with melanin NPs (diameter ≈ 15 nm) loading even as low as 1 wt % blocks most ultraviolet light below 340 nm and still keeps high visible light transparency (83%) in the visible spectrum. More importantly, because of the excellent photoprotection and radical scavenging capabilities of melanin, the resulting polymer nanocomposite exhibits outstanding photostability. In effect, such fantastic melanin NPs is promising for applications in various optical materials.

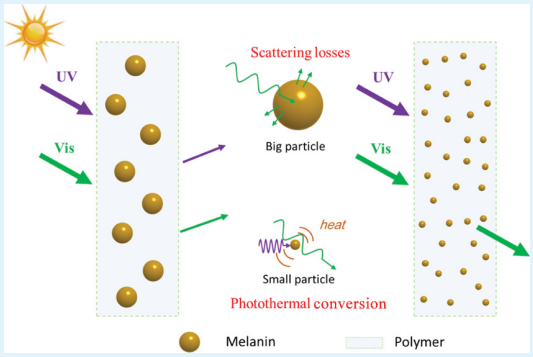

KEYWORDS: *melanin, polymer, UV-shielding, transparency, photostability*

INTRODUCTION

Ultraviolet (UV) radiation has been used in a wide variety of fields such as biomedical materials, cosmetic, optical sensors, polymer modification, and so on. However, it is well-known that overexposure to UV light would harm human health.[1] Because of its high-energy, UV light with short wavelengths can also destroy the covalent bonds in organic materials, causing a series of undesirable degradation effects on materials. To avoid the harmful effect of UV irradiation, it is essential to design effective UV-shielding optical materials.

Among the materials used in the optical materials field, polymers blended with fillers have been considered as one of the most effective methods and found numerous applications in household, industry, and military field. In the last decade, many organic UV absorbers and inorganic oxides have been reported to improve the UV-shielding performance of polymers.[2−4] Organic UV absorbers such as benzophenones or triazines can dissipate UV light. Inorganic oxides (e.g., titanium dioxide, zinc oxide, silicon dioxide, and aluminium oxide) attenuate UV light through bandgap absorption and scattering of light. However, conventional organic absorbers always suffer from photodegradation, migration, or aggregation when embedded in polymer matrices.[5,6] The majority of inorganic oxides usually show side effects, such as photocatalytic property upon UV light absorption, which could induce photodegradation of polymer matrices simultaneously.[5,7−9] Another way of preparing UV protective polymer materials is by applying high concentrations of protective coating on the material. Nevertheless, the shortcoming is the expensive secondary step during the production process. Recently, ZrO_2−SiO_2 photonic crystal fillers have been fabricated by layer-by-layer deposition. Unfortunately, the visible light transparency of the film was not as good as expected when it came to the complete UV-shielding performance.[10−12] Besides these organic and inorganic oxide materials, nitrogen-doped graphene sheets were used as UV absorbers.[13]

Melanin is a special kind of biomacromolecule that is widely found in nature and display many useful properties, such as adsorption of UV radiation (photoprotection), coloration, photothermal conversion, and free radical scavenging properties.[14−19] The chemical structure and properties of melanin have been already proposed; however, the exact knowledge of its structure, especially at the molecular level, remains poorly documented. In general, melanin owns many reactive groups, such as −NH− and −OH.[20,21] There are two methods to prepare melanin models: natural melanin model and synthetic melanin model. The natural melanin model has been obtained from a biological source. Synthetic melanin model is obtained by chemical oxidation of dopamine or enzymatic oxidation of precursor molecules.[22] Both natural and synthetic melanin show similar physical and chemical properties.[23] In fact, exploiting the many desirable of functional properties of melanin to augment the properties of other materials still remains largely unexplored.

Received: February 12, 2018
Accepted: March 26, 2018
Published: March 26, 2018

DOI: 10.1021/acsami.8b02658
ACS Appl. Mater. Interfaces 2018, 10, 13100−13106

Bisphenol A polycarbonate (PC) as engineering plastic, is used in many fields. PC would degrade and display losses in mechanical properties and yellowing because of UV light.[24,25] It is known that blending of traditional UV absorbers, quenchers, and radical scavengers can protect PC but are not very effective in preventing the degradation of the surface of films. In this case, the high content of stabilizers is necessary. Thus, the exploration of UV-shielding and photostability PC composites is highly desirable by simple methods.

In this paper, natural melanin extracted from *Sepia officinalis* and synthetic melanin derived from the oxidation of dopamine have been used to enhance the UV-shielding properties of PC. Introduction of fillers into transparent polymers, even at low contents, often leads to opaque composites because of light scattering caused by the fillers because of the refractive index mismatch between fillers and polymer matrices.[26] Taking the above into account, the visible light transparency property of the PC nanocomposite films was further studied. The results demonstrated that the shielding and visible light transparency behaviors of nanocomposite were strongly size-dependent. As the particle size decreased, the PC nanocomposite exhibited high short-wavelength shielding, high visible light pass, and photostability properties.

EXPERIMENTAL SECTION

Materials. Bisphenol A PC was obtained from Sabic Innovative Plastic. Dopamine hydrochloride (98%) and rhodamine B (RhB, >99%) were purchased from Aladdin. Titania (TiO_2) nanoparticles (NPs) (P25) with a size of approximately 25 nm were purchased from Sigma-Aldrich.

Extraction of Natural Melanin NPs. Natural melanin was separated from ink of *S. officinalis*. After several washing and centrifugation (10 000 rpm for 30 min) processes, a clean natural melanin was obtained.

Size Control of Synthetic Melanin NPs. The synthesis of melanin NPs with a diameter of ∼240 and ∼80 nm is given. Melanin NPs were synthesized by oxidation of dopamine following the procedure outlined by Lee et al.[15] Dopamine hydrochloride (0.18 g) and NaOH solution (0.76 mL, 1 N) were dissolved in deionized water (90 mL), and stirred at 20 and 50 °C, respectively. After 5 h, synthetic melanin NPs were purified repeatedly by centrifugation (10 000 rpm, 30 min) and washed with water several times until the supernatant was clear. Then, the sample was dried in vacuum for 24 h to obtain synthetic melanin (melanin-240 and melanin-80). Melanin NPs with a diameter of ∼15 nm (melanin-15) were prepared according to our previous report; dopamine hydrochloride (0.18 g) and NaOH solution (0.9 mL, 1 N) were added into poly(vinyl alcohol) solution (0.1 wt %, 90 mL) and stirred at 50 °C for 5 h. Melanin NPs were purified repeatedly through centrifugation (18 000 rpm, 30 min) and washed with water several times until the supernatant was clear. Then, the sample was dried in vacuum for 24 h to obtain synthetic melanin.[21]

Preparation of Polymer Nanocomposites. Melanin NPs were dispersed in a 20 wt % PC in cyclohexanone solution (100 mL). Then, films (thickness of 100 μm) were prepared by the casting method and dried in vacuum oven at 60 °C for 24 h to eliminate the solvent completely.

UV-Shielding Performance of PC Nanocomposite Films. The degradation of RhB (50 mL) with TiO_2 (25 mg) under a high-pressure mercury lamp (150 W) was applied to measure the UV-shielding properties of films. RhB solution was added into a beaker and covered with films. The air gap between the polymer film and the solution was about 4 cm. The distance between the lamp and the film was about 10 cm. The absorbance at 552 nm of solution was determined.

UV-Ageing Test Procedure. The UV-aging test was performed in a chamber with a UV lamp (RPR-200 Rayonet, irradiation wavelength of 365 nm) with an light intensity of 90 W/m^2 at the center of the reactor.

Characterizations. The morphologies of melanin were obtained on scanning electron microscopy (SEM, Hitachi S4800) and transmission electron microscopy (TEM, Philips TECNAI 20), respectively. The mean diameter and size distribution of melanin NPs were measured using dynamic light scattering (DLS) measurements (ALV/DLS/SLS-5022F, Germany). UV−vis spectra were observed by a TU-1901 spectrophotometer. The degraded films were detected by using Fourier-transform infrared spectroscopy (FTIR). The surface topography of films was investigated using an atomic force microscope (AFM, Bruker MultiMode 8).

RESULTS AND DISCUSSION

Sepia eumelanin from cuttlefish are used as a standard for natural melanin. SEM and TEM images reveal that the natural melanin NPs are roughly spherical (average diameter of 150 nm) (Figure 1a,b).

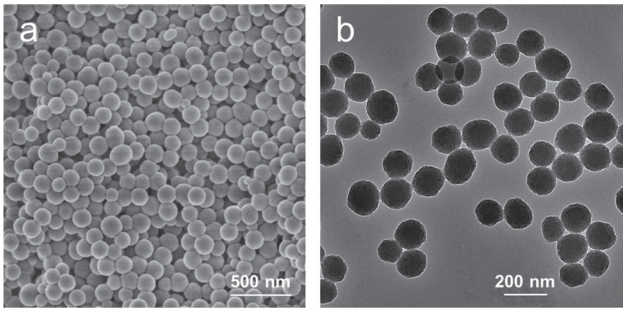

Figure 1. (a) SEM and (b) TEM images of natural melanin (sepia eumelanin).

The optical properties of PC/natural melanin nanocomposite films were measured using UV−vis spectroscopy. The pure PC film shows no obvious absorption in the region 300−400 nm. On incorporation of natural melanin, the spectrum of PC nanocomposite shows absorption below 400 nm, and the shoulder absorption becomes stronger with the increasing natural melanin content (Figure 2a). The UV-shielding properties of the nanocomposite film were evaluated by UV−vis transmittance spectra. The pure PC film demonstrates little absorption between 270−350 nm and only blocked deep UV light below 270 nm. By contrast, the PC nanocomposite film with the addition of 0.5 wt % natural melanin NPs shows about 50% blocking in the region of 300 nm. When the natural melanin content increased to 2 wt %, the film could almost shield the UV radiation below 280 nm, whereas the transparency at 550 nm is only about 40% (Figure 2b).

As shown in Figure 2b, the shielding property can be easily improved through increasing the natural melanin content. However, it is a challenge to get a good balance between the shielding property and visible light transparency. A high visible light transparency is the important premise for optical materials. The properties of polymer composites depend on the shape of the filler particles and the dispersion of fillers in the matrix. To our knowledge, the particle size of melanin NPs can be simply controlled by tuning several synthetic conditions. By mimicking natural melanin, synthetic melanin NPs with different sizes were designed. The preparation process of synthetic melanin is illustrated in Figure 3. As indicated in the SEM (Figure 3), the synthetic melanin NPs with three different sizes were obtained. All NPs display smooth spherical shapes. At the same time, the size of each sample was characterized by TEM and DLS (Figure 4). The three synthetic melanin NPs

DOI: 10.1021/acsami.8b02658
ACS Appl. Mater. Interfaces 2018, 10, 13100−13106

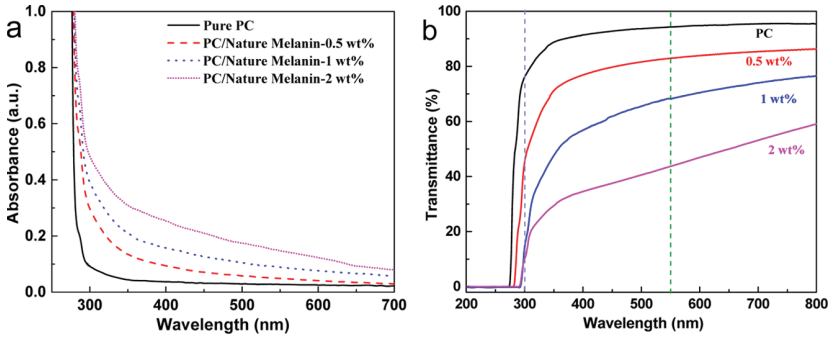

Figure 2. (a) UV−vis absorption spectra and (b) transmittance spectra of nanocomposite films with different natural melanin content.

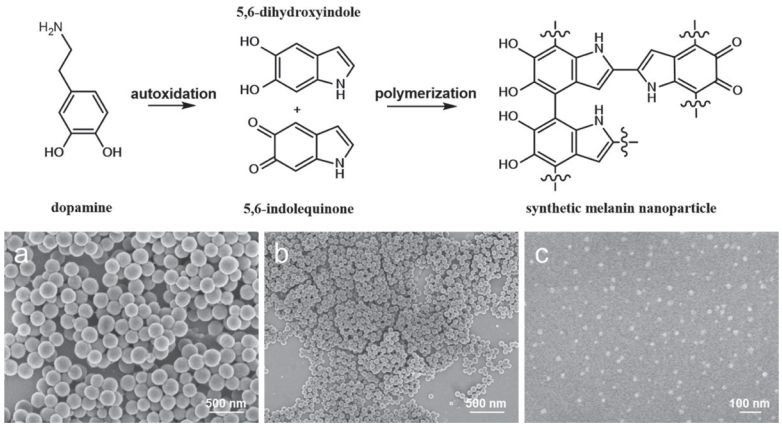

Figure 3. SEM images of synthetic melanin NPs with different particle sizes: (a) melanin-240, (b) melanin-80, and (c) melanin-15 nm. (The inset shows the fabrication of synthetic melanin.)

show relatively narrow distribution, and the diameters were estimated to be 240, 80, and 15 nm.

The FTIR spectra of natural and synthetic melanin are shown in Figure 5a. No substantial differences are observed between them, indicating similar functional groups. Both spectra display a broad band at 3400 cm^{-1}, attributed to stretching vibrations of −OH and $-NH_2$ groups. As may be expected, the absorption spectrum of synthetic melanin shows a broad absorbance increase from 700 to 200 nm similar to that of natural melanin (Figure 5b). Those broad spectra normally are related to the photoprotective function. Synthetic melanin NPs with a small size shows an additional peak at 280 nm, which is most likely due to the quinone in the melanin backbone reverting to a catechol.[27] In addition, the particle size of the synthetic melanin NPs was still kept after 500 h of UV exposure (Figure 6).

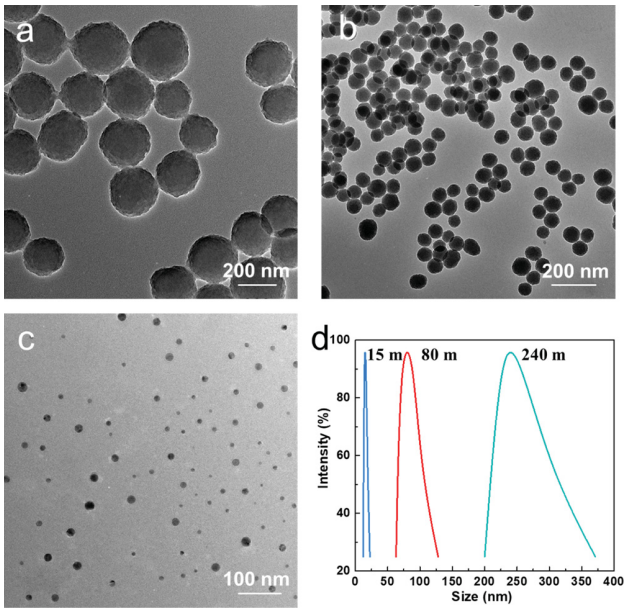

Figure 4. TEM images of synthetic melanin NPs with an average particle diameter of (a) 240, (b) 80, and (c) 15 nm. (d) DLS of NPs.

Furthermore, the effect of the melanin particle size on optical properties was investigated. Figure 7a shows the UV−vis transmittance spectra of PC nanocomposite films with only 1 wt % melanin NPs loading. It is found that the UV-shielding and visible light transparency depend on the size of melanin NPs obviously. When melanin NPs with a size of 240 nm was incorporated, the nanocomposite film could only block the UV radiation below 270 nm, and the visible light transparency deceases to 50%. Interestingly, with the particle size decreasing from 240 to 15 nm, the UV-shielding performance improves, all of the UV light below 340 nm is efficiently blocked, whereas visible light transparency is still very high (83%), being close to that of the pure PC. For discrete spherical particles embedded in a polymer matrix, the decrease of visible light transparency because of light scattering can be described by eq 1[28]

DOI: 10.1021/acsami.8b02658
ACS Appl. Mater. Interfaces 2018, 10, 13100−13106

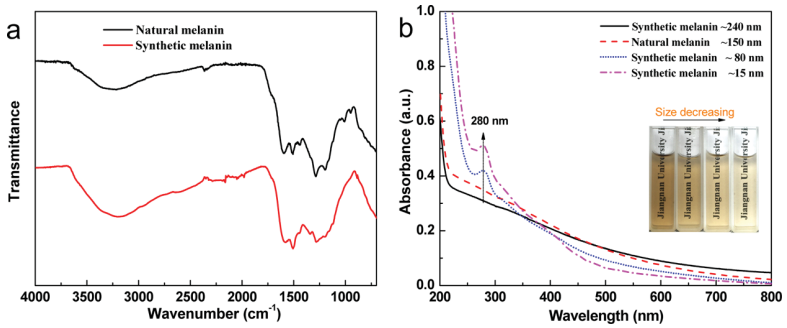

Figure 5. (a) FTIR characterization and (b) UV−vis absorbance of natural and synthetic melanin (20 μg mL^{-1}). (The inset b: photograph of melanin dispersed in H_2O.)

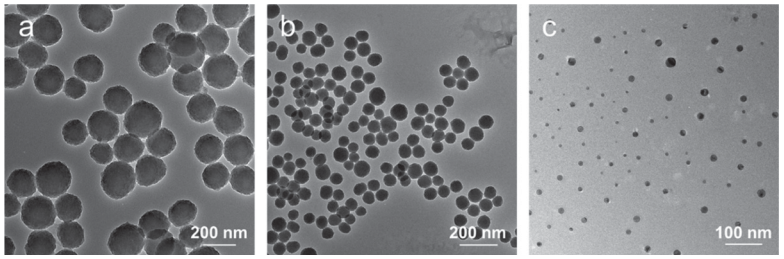

Figure 6. TEM images of synthetic melanin NPs after 500 h of UV exposure (a) melanin-240, (b) melanin-80, and (c) melanin-15 nm.

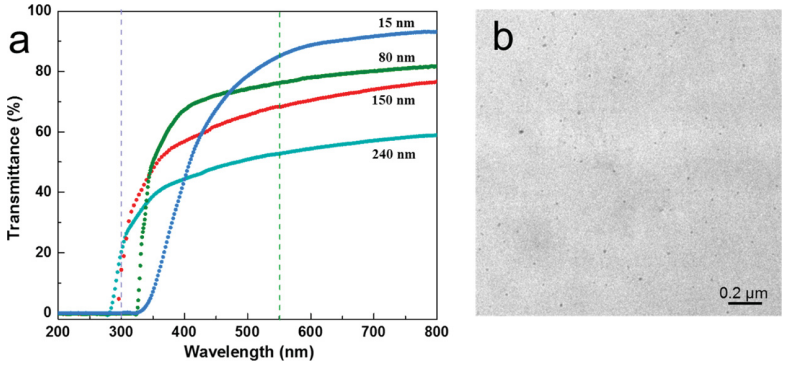

Figure 7. (a) UV−vis light transmittance spectra of PC/melanin nanocomposites. (b) TEM image for PC/melanin-15 (1 wt %) nanocomposite.

$$\frac{I}{I_0} \approx \exp\left[\frac{-3V_p x r^3}{4\lambda^4}\left(\frac{n_p}{n_m} - 1\right)\right] \quad (1)$$

where x is the optical path-length, V_p is the particle volume fraction, r is the particle radius, λ is the light wavelength, and n_p and n_m are refractive indices of the particles and matrix, respectively. Equation 1 shows that the light intensity reduces dramatically as r increases. For a small particle, light scattering is significantly reduced and thus the visible light transparency of the polymeric material is retained. Generally, as the particle size decreases, particle agglomeration becomes severe and deteriorates the particle dispersion. Such agglomerates can persist in the composite and scatter visible light.[26,29] Figure 7b shows TEM of the PC/melanin-15 nanocomposite. Fortunately, it is obvious to see that the melanin NPs are individually dispersed in the PC matrix. The good dispersion of melanin NPs is an additional factor that nearly nullifies the Rayleigh scattering losses, especially in the visible region, thereby retaining the optical clarity. As shown in Figure 8, use of big particles bring about large visible light shielding and scattering light. It is hard

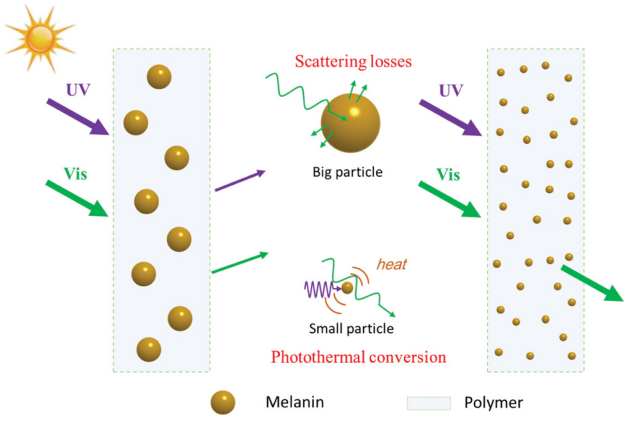

Figure 8. Schematic representation of the influence of the melanin particle size on optical properties of polymer nanocomposites.

to keep the high transparency of the polymer because of light scattering caused by the mismatch of the refractive index between the NPs and the polymer. By contrast, highly

DOI: 10.1021/acsami.8b02658
ACS Appl. Mater. Interfaces 2018, 10, 13100−13106

dispersed melanin NPs have a small size and high accessible surface areas in the polymer matrix and make it easy for short-wavelength (UV light) to be absorbed and long-wavelength (visible light) to pass (Figure 8).

The UV-shielding performance of films with different particle sizes of melanin was further examined. RhB solution protected with pure PC or PC/melanin nanocomposite films were measured under the same conditions. As shown in Figure 9,

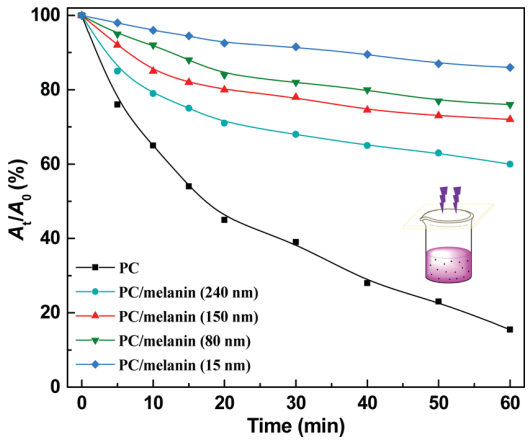

Figure 9. Photodegradation of RhB solution protected by PC and PC/melanin nanocomposite films. The thickness of film is 100 ± 5 μm.

after irradiation for 60 min, RhB under the protection of pure PC shows a loss 80%, while the RhB solution protected by the PC/melanin-240 nanocomposite film shows a decrease of 40%. The photoprotective efficiency increases with the decreasing of the size of melanin NPs. For RhB solution protected by PC/melanin-5, only about 15% of solution degraded, demonstrating outstanding UV-shielding efficiency.

To investigate the photostability of PC nanocomposite films, attenuated total reflection (ATR)−FTIR were recorded. Figure 10a shows the ATR−FTIR spectra of PC and PC/melanin-15 nanocomposite film after UV irradiation with different times. The change of the absorbance at 3800−3200 and 1900−1500 cm^{-1} during UV irradiation reflects the formation of hydroperoxides and alcohols and carbonyl photodegradation compounds (such as ketones and carboxylic acid), respectively.[30,31] As photodegradation proceeds, the hydroxyl and carbonyl absorption bands broaden with the increasing irradiation time for pure PC. By contrast, there is no change at the carbonyl absorption for PC/melanin nanocomposite even with 500 h irradiation, only a little higher absorption at 3350 cm^{-1} (Figure 10b). Hence, it is obvious that melanin is against the photodegradation. In PC the reasons, underlying the degradation, has been ascribed to photo-fries rearrangement and main-chain photo-oxidation. However, as a result, the photodegradation with longer wavelengths (365 nm) can mainly be due to photo-oxidation.[32] Melanin NPs can dissipate UV light via converting the absorbed energy into heat. On the other hand, as a radical scavenger, it inhibits the creation of reactive species or the sublimation of reaction products.

The degradation of layer surface of films was analyzed with AFM. As can be seen in Figure 11, both pure PC and PC/melanin nanocomposite films have a plain and smooth surface before irradiation. As one immediately notices, UV irradiation results in obvious changes, hill-like structures and pits appear in the surface of the pure PC. This phenomenon is generally due to the migration of low molecular weight products in the gas phase and evaporation of products during photodegradation.

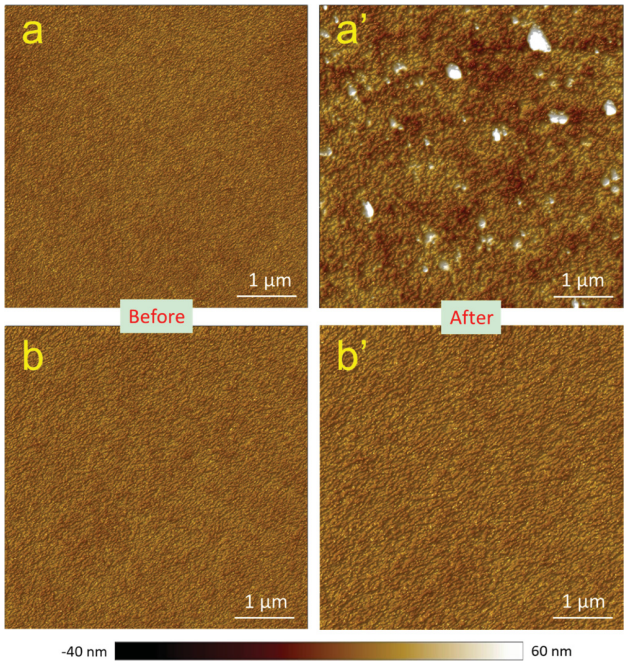

Figure 11. AFM images of (a,a′) pure PC and (b,b′) PC/melanin-15 (1 wt %) nanocomposite films before and after exposure to the UV irradiation.

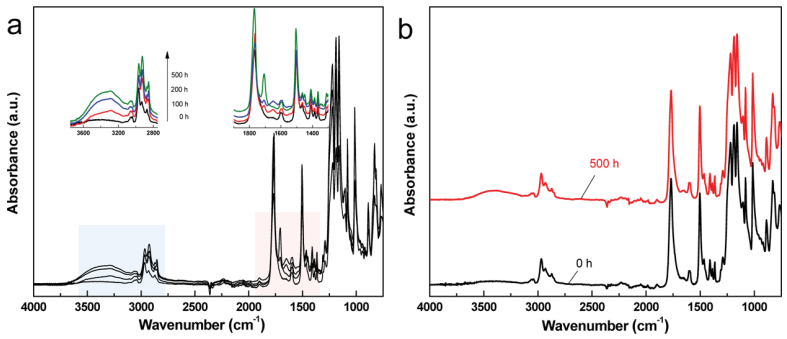

Figure 10. ATR−FTIR absorption spectra of (a) pure PC with different times of UV irradiation (the inset a: selected area). (b) PC/melanin (15 nm)-1 wt % film before and after 500 h of UV irradiation.

DOI: 10.1021/acsami.8b02658
ACS Appl. Mater. Interfaces 2018, 10, 13100−13106

Comparing the pure PC, there is no systematic change in the surface topology of PC nanocomposites after irradiation. This result again strongly points to a very much improved photostability of the nanocomposites.

CONCLUSIONS

In summary, natural melanin and synthetic melanin NPs were systematically investigated for its potential optical applications in the polymer matrix. The influences of the melanin particle size on the optical properties of the polymer nanocomposite films were further studied. Interestingly, the significant short-wavelength shielding and high visible light pass properties of polymer nanocomposite were easy obtained via tuning the melanin particle size. Decreasing the melanin particle size leads to an increased UV-shielding and visible light transparency properties. For a small particle, light scattering is significantly reduced and thus the visible light transparency of the polymeric material is retained. More importantly, adding only 1 wt % melanin NPs with a size of 15 nm can endow the polymer with significant photostability and performance. Therefore, melanin will provide a novel method to fabricate optical polymer materials.

AUTHOR INFORMATION

Corresponding Author

*E-mail: wfdong@jiangnan.edu.cn. Phone: +86-510-8532-6290. Fax: +86-510-8591-7763.

ORCID

Yang Wang: 0000-0001-7875-9111

Weifu Dong: 0000-0002-7432-8362

Notes

The authors declare no competing financial interest.

ACKNOWLEDGMENTS

This work was supported by National Natural Science Foundation of China (51373070), the Fundamental Research Funds for the Central Universities (JUSRP51624A), MOE & SAFEA, 111 Project (B13025), the scholarship from China Scholarship Council (CSC) under the grant CSC N201706790065, the Innovation Project for College Graduates of Jiangsu Province (KYLX16_0784), Joint Pre-research Foundation of Ministry of Education of China (6141A02022228), and National First-Class Discipline Program of Light Industry Technology and Engineering (LITE2018-19).

REFERENCES

(1) Dickerson, R. R.; Kondragunta, S.; Stenchikov, G.; Civerolo, K. L.; Doddridge, B. G.; Holben, B. N. The impact of aerosols on solar ultraviolet radiation and photochemical smog. *Science* **1997**, *278*, 827−830.

(2) Wang, Y.; Xiang, C.; Li, T.; Ma, P.; Bai, H.; Xie, Y.; Chen, M.; Dong, W. Enhanced thermal stability and UV-shielding properties of poly(vinyl alcohol) based on esculetin. *J. Phys. Chem. B* **2017**, *121*, 1148−1157.

(3) Zayat, M.; Garcia-Parejo, P.; Levy, D. Preventing UV-light damage of light sensitive materials using a highly protective UV-absorbing coating. *Chem. Soc. Rev.* **2007**, *36*, 1270.

(4) Wang, Y.; Li, T.; Ma, P.; Bai, H.; Xie, Y.; Chen, M.; Dong, W. Simultaneous enhancements of UV-shielding properties and photostability of poly(vinyl alcohol) via incorporation of sepia eumelanin. *ACS Sustainable Chem. Eng.* **2016**, *4*, 2252−2258.

(5) Calvo, M. E.; Castro Smirnov, J. R.; Míguez, H. Novel approaches to flexible visible transparent hybrid films for ultraviolet protection. *J. Polym. Sci., Part B: Polym. Phys.* **2012**, *50*, 945−956.

(6) Subramani, N. K.; Kasargod Nagaraj, S.; Shivanna, S.; Siddaramaiah, H. Highly flexible and visibly transparent poly(vinyl alcohol)/calcium zincate nanocomposite films for UVA shielding applications as assessed by novel ultraviolet photon induced fluorescence quenching. *Macromolecules* **2016**, *49*, 2791−2801.

(7) Wang, X.; Zhou, S.; Wu, L. Fabrication of Fe^{3+} doped Mg/Al layered double hydroxides and their application in UV light-shielding coatings. *J. Mater. Chem. C* **2014**, *2*, 5752−5758.

(8) Yu, J. C.; Yu; Ho; Jiang; Zhang. Effects of F^- doping on the photocatalytic activity and microstructures of nanocrystalline TiO_2 powders. *Chem. Mater.* **2002**, *14*, 3808−3816.

(9) Li, D.; Qian, L.; Feng, Y.; Feng, J.; Tang, P.; Yang, L. Co-intercalation of acid red 337 and a UV absorbent into layered double hydroxides: enhancement of photostability. *ACS Appl. Mater. Interfaces* **2014**, *6*, 20603−20611.

(10) Smirnov, J. R. C.; Calvo, M. E.; Míguez, H. Selective UV reflecting mirrors based on nanoparticle multilayers. *Adv. Funct. Mater.* **2013**, *23*, 2805−2811.

(11) Núñez-Lozano, R.; Pimentel, B.; Castro-Smirnov, J. R.; Calvo, M. E.; Míguez, H.; Cueva-Méndez, G. d. l. Biocompatible films with tailored spectral response for prevention of DNA damage in skin cells. *Adv. Healthcare Mater.* **2015**, *4*, 1944−1948.

(12) Jang, S.; Kang, S. M.; Choi, M. Multifunctional moth-eye TiO_2/PDMS pads with high transmittance and UV filtering. *ACS Appl. Mater. Interfaces* **2017**, *9*, 44038−44044.

(13) He, W.; Lu, L. Revisiting the structure of graphene oxide for preparing new-style graphene-based ultraviolet absorbers. *Adv. Funct. Mater.* **2012**, *22*, 2542−2549.

(14) Wang, Y.; Su, J.; Li, T.; Ma, P.; Bai, H.; Xie, Y.; Chen, M.; Dong, W. A novel UV-shielding and transparent polymer film: when bioinspired dopamine−melanin hollow nanoparticles join polymers. *ACS Appl. Mater. Interfaces* **2017**, *9*, 36281−36289.

(15) Ju, K.-Y.; Lee, Y.; Lee, S.; Park, S. B.; Lee, J.-K. Bioinspired polymerization of dopamine to generate melanin-like nanoparticles having an excellent free-radical-scavenging property. *Biomacromolecules* **2011**, *12*, 625−632.

(16) Shanmuganathan, K.; Cho, J. H.; Iyer, P.; Baranowitz, S.; Ellison, C. J. Thermooxidative stabilization of polymers using natural and synthetic melanins. *Macromolecules* **2011**, *44*, 9499−9507.

(17) Dong, W.; Wang, Y.; Huang, C.; Xiang, S.; Ma, P.; Ni, Z.; Chen, M. Enhanced thermal stability of poly(vinyl alcohol) in presence of melanin. *J. Therm. Anal. Calorim.* **2014**, *115*, 1661−1668.

(18) Wang, Y.; Yuan, H.; Ma, P.; Bai, H.; Chen, M.; Dong, W.; Xie, Y.; Deshmukh, Y. S. Superior performance of artificial nacre based on graphene oxide nanosheets. *ACS Appl. Mater. Interfaces* **2017**, *9*, 4215−4222.

(19) d'ischia, M.; Napolitano, A.; Pezzella, A.; Meredith, P.; Sarna, T. Chemical and structural diversity in eumelanins: unexplored bio-optoelectronic materials. *Angew. Chem., Int. Ed.* **2009**, *48*, 3914−3921.

(20) Wang, Y.; Li, T.; Wang, X.; Ma, P.; Bai, H.; Dong, W.; Xie, Y.; Chen, M. Superior performance of polyurethane based on natural melanin nanoparticles. *Biomacromolecules* **2016**, *17*, 3782−3789.

(21) Wang, Y.; Wang, Z.; Ma, P.; Bai, H.; Dong, W.; Xie, Y.; Chen, M. Strong nanocomposite reinforcement effects in poly(vinyl alcohol) with melanin nanoparticles. *RSC Adv.* **2015**, *5*, 72691−72698.

(22) Liu, Y.; Ai, K.; Liu, J.; Deng, M.; He, Y.; Lu, L. Dopamine-melanin colloidal nanospheres: an efficient near-infrared photothermal therapeutic agent for in vivo cancer therapy. *Adv. Mater.* **2013**, *25*, 1353−1359.

(23) Liu, Y.; Ai, K.; Lu, L. Polydopamine and its derivative materials: synthesis and promising applications in energy, environmental, and biomedical fields. *Chem. Rev.* **2014**, *114*, 5057−5115.

(24) Diepens, M.; Gijsman, P. Photostabilizing of bisphenol A polycarbonate by using UV-absorbers and self protective block copolymers based on resorcinol polyarylate blocks. *Polym. Degrad. Stab.* **2009**, *94*, 1808−1813.

DOI: 10.1021/acsami.8b02658
ACS Appl. Mater. Interfaces 2018, 10, 13100−13106

(25) Diepens, M.; Gijsman, P. Photo-oxidative degradation of bisphenol A polycarbonate and its possible initiation processes. *Polym. Degrad. Stab.* **2008**, *93*, 1383−1388.
(26) Li, Y.-Q.; Fu, S.-Y.; Yang, Y.; Mai, Y.-W. Facile synthesis of highly transparent polymer nanocomposites by introduction of core−shell structured nanoparticles. *Chem. Mater.* **2008**, *20*, 2637−2643.
(27) Guin, T.; Cho, J. H.; Xiang, F.; Ellison, C. J.; Grunlan, J. C. Water-based melanin multilayer thin films with broadband UV absorption. *ACS Macro Lett.* **2015**, *4*, 335−338.
(28) Novak, B. M. Hybrid Nanocomposite Materials—between inorganic glasses and organic polymers. *Adv. Mater.* **1993**, *5*, 422−433.
(29) Gu, Z.-Z.; Kubo, S.; Qian, W.; Einaga, Y.; Tryk, D. A.; Fujishima, A.; Sato, O. Varying the optical stop band of a three-dimensional photonic crystal by refractive index control. *Langmuir* **2001**, *17*, 6751−6753.
(30) Rivaton, A.; Sallet, D.; Lemaire, J. The photochemistry of bisphenol-A polycarbonate reconsidered. *Polym. Photochem.* **1983**, *3*, 463−481.
(31) Lemaire, J.; Gardette, J.-L.; Rivaton, A.; Roger, A. Dual photochemistries in aliphatic polyamides, bisphenol A polycarbonate and aromatic polyurethanes−A short review. *Polym. Degrad. Stab.* **1986**, *15*, 1−13.
(32) Diepens, M.; Gijsman, P. Photodegradation of bisphenol A polycarbonate. *Polym. Degrad. Stab.* **2007**, *92*, 397−406.

DOI: 10.1021/acsami.8b02658
ACS Appl. Mater. Interfaces 2018, 10, 13100−13106